Ballistic energy transfer in dielectric Ar crystals

2001 J. Phys.: Condens. Matter 13 4323

(http://iopscience.iop.org/0953-8984/13/19/312)

INSTITUTE OF PHYSICS PUBLISHING JOURNAL OF PHYSICS: CONDENSED MATTER

J. Phys.: Condens. Matter **13** (2001) 4323–4339 www.iop.org/Journals/cm PII: S0953-8984(01)19019-3

Ballistic energy transfer in dielectric Ar crystals

A Cenian[1,2] **and H Gabriel**[1]

[1]Institut für Theoretische Physik, Freie Universität Berlin, Arnimallee 14, 14195 Berlin, Germany
[2]Institute of Fluid-Flow Machines, Polish Academy of Sciences, 80-952 Gdańsk, ul. Fiszera 14, Poland

E-mail: cenian@imp.gda.pl and gabriel@physik.fu-berlin.de

Received 14 November 2000, in final form 19 February 2001

Abstract

The results of a molecular dynamics study of the supersonic propagation of femtosecond-energy pulses in a three-dimensional dielectric Ar crystal are presented. Within the first few picoseconds following pulse excitation, a significant ballistic contribution to heat transfer is observed which prevents the system from showing the features of normal heat conduction, i.e. the existence of finite temperature gradients and the requirement that heat conductivity be an intensive quantity. It is shown that the ballistic energy-transfer part exhibits similarities with solitary pulses as studied by G Leibfried and M Toda independently; they are collisionally stable and the pulse velocity is proportional to the square root of the tranferred energy. The ballistic current may thus be considered as a sequence of Leibfried–Toda (LT) solitons travelling through a dissipative medium. The current decreases with the lattice temperature and with the distance from the heat source. It may, however, contribute to heat transfer even at distances roughly 150 lattice constants away from the excitation site. The ballistic, soliton-like propagation along close-packed directions is highly directional and hardly compatible with the spherical symmetry of a Fourier heat current emanating from a point heat source. Radial and lateral anisotropy of the ballistic heat current is shown to be present during a time span of several picoseconds. A simplified formula for the ballistic energy transfer is proposed. Furthermore, we have proven that coherent many-atom excitation can be devised in such a way that the lifetime of the LT solitons is enhanced. The conditions to optimize solitary pulse stability are discussed.

1. Introduction

There is growing evidence that heat conduction in micro-size dielectric crystals proceeds simultaneously via two very different mechanisms: diffusive and ballistic [1–6]. Starting with the early investigations of Born [7], Debye [8] and Peierls [9], much effort was put into defining the necessary properties of a system to obey Fourier's law (diffusive conduction) valid in macroscopic dielectric solids [1–3, 6–27]. Attention was paid to the role of nonlinearity,

structural and isotopic disorder as well as dimensionality. As to the latter, it is known that systems with higher dimensions fulfil the necessary conditions for heat diffusion more easily [13, 14]. Concerning 1D systems, a series of recent investigations has attempted to clarify under which conditions Fourier's law of heat conduction is obeyed [13–23]. It is well established that the thermal conductivity diverges—in the thermodynamic limit—in any integrable 1D system. Recently, an important rigorous proof was given by Prosen and Campbell [15] that for a classical 1D system with arbitrary adjacent site–site interactions, conservation of total momentum implies anomalous conductivity provided the average pressure vanishes. Numerical studies of Hu *et al* [16] and of Hatano [17] clarify that anomalous heat conductivity in 1D systems is strongly related to the presence of translational invariance. In contrast, normal thermal conductivity was found in several systems where this symmetry is broken due to the presence of external on-site potentials (e.g. the ding-a-ling [12], the Frenkel–Kontorowa [16], and the ding-dong model [18]). The determinant role of an external potential for normal thermal conduction to occur was recently presented by Hu *et al* [19] who studied the ϕ^4 model (exhibiting normal thermal conductivity κ), and the Fermi–Pasta–Ulam model [10] (where κ diverges). Tsironis *et al* discussed [20] heat conductivity in a harmonically coupled chain with three different anharmonic on-site potentials paying particular attention to the role of breathers. Note, however, the results obtained in [21, 22] showing that absence of an on-site potential does not necessarily lead to a divergent thermal conductivity. Both groups of investigators studied a linear chain of coupled rotors. Although momentum is conserved, the conductivity is finite. This is explained by excitation of stationary localized rotational modes capable of successively locking and releasing the heat flux in [21] and is traced back to the occurrence of jumps through barriers in [22].

Since the present paper deals with energy transfer in a perfect crystal, the effect of disorder on the thermal conductivity will not be discussed here. Instead, we refer to a recent contribution by Li *et al* [23], where a list of references relevant for the topic can be found and in which a numerical study of heat transfer in mass-disordered harmonic and anharmonic 1D lattices is presented.

Nonlinear and chaotic systems do not guarantee the necessary conditions for normal thermal conduction to occur [10, 6, 24]. It has been shown in [3] and [6] that in a system evolving along a chaotic trajectory, diffusive and ballistic heat transport can coexist. This has been deduced from the size dependence of the thermal conductivity in 1D and 2D chains interacting, e.g. via Toda, Fibonacci or harmonic+quartic term potentials. The effect is found if the system extends in the direction of heat propagation over less than 150 crystal sites [3]. Nishiguchi *et al* [3] have postulated that the anomalous rise of the conductivity in dielectric crystals found for large temperature gradients is due to KdV solitons. Already Toda [25] had pointed out that solitons may increase the heat conductivity in dielectric crystals. In regular, ordered Toda lattices they propagate without any hindrances (dissipation) contributing to vanishing temperature gradients and infinite conductivity as in linear chains [26]. In disordered crystals they inhibit heat transfer as they are possibly more robust against the scattering centres than normal phonon modes.

The anomalous dependence of the heat conductivity on lattice size disappears for larger systems [3], i.e. the solitons (ballistic current) undergo dissipation. Only when solitons lose most of their energy at some distance from the warmer end of the lattice, the diffusive part of the heat current dominates, Fourier's law of heat transfer is applicable and heat conductivity becomes an intensive quantity. This dependence on system size (discussed also by Jackson and Mistriotis [1] in the case of a diatomic Toda lattice), may in some cases be interpreted as a failure of any system to show normal conductivity. However, we believe that the coexistence of ballistic and diffusive heat currents is one of the pre-eminent features of most microscale

systems. At macroscopic size they may reveal normal conductivity. The present paper concentrates on the microscopic investigation of the ballistic energy transfer in a 3D rare-gas crystal to a good approximation realistically described by using empirical pair potentials. We will show that there is a strong ballistic contribution to energy transfer on a microscopic scale. Later, after a few picoseconds of heat-pulse propagation through the crystal the system slowly shifts to 'nearly' normal conduction.

The nature of the ballistic part of the heat current was studied extensively for the case of energy transfer emanating from a thermal spike in the bulk. The thermal excitation may be produced by photodissociation of guest molecules in crystals or nonradiative exciton quenching in rare-gas solids [34, 4, 38, 5, 27]. The energy, initially localized at a single excited atom of the crystal, is transferred along close-packed directions [31, 33] in the form of shock pulses [34, 4]. This ultra-fast (supersonic) and efficient way of energy transfer prevents local overheating and melting as suggested in [30]. The solitary, nonlinear character of these pulses was proven in [5]. In real systems ballistic transfer can play a crucial role in microphysical processes such as cage exit [30], sputtering [31] and cluster collisions [32]. Experiments on the photodissociation of F_2 in a Kr matrix by Kunttu *et al* [35] or on so-called 'ballistical phonons' created by short laser pulses in crystals [29] also point to the relevance of ballistic transfer processes.

In the present paper we aim to investigate the solitary character of supersonic energy pulses, their dissipation in an Ar matrix as well as their relation to heat (energy) transfer. In section 2 we describe the main features of the models used. Section 3 considers the Toda and Leibfried solitons and their relation to the process of energy transfer from the 'thermal spike'. The dissipation of solitary shock pulses is discussed in section 4 which includes, for the convenience of the reader, the main results of our previous work [38] discussed in the light of new data. A simplified formula for ballistic energy (heat) current is proposed and the applicability of Fourier description is discussed. In section 5 we discuss the dissipation behaviour of solitary shock pulses in systems with a one-dimensional array of impurity atoms excited under conditions that differ from those of a thermal spike.

2. Model description

The energy transfer following local excitation was studied by using a molecular dynamics (MD) procedure based on a Verlet-type algorithm. The equations of motion were solved for 2916 Ar atoms in a cubic box $9 \times 9 \times 9\ a_{\mathrm{Ar}}^3$ (a_{Ar} lattice constant of Ar), and 2520 atoms in a tetragonal box $36 \times 7 \times 5\ R_{\mathrm{e}}^3$ ($R_{\mathrm{e}} = a_{\mathrm{Ar}}/\sqrt{2}$). The pair potential of Azis *et al* [36] was chosen.

The crystallographic [110] direction was chosen to be the x-axis in the second case. The tetragonal box was used to study shock pulse propagation during the first 1.5–2 ps, without being affected by the periodic boundary conditions. Using the nearest-neighbour distance $R_{\mathrm{e}} = 3.7565$ of the Ar crystal, we were able to study pulses that traverse a distance of ~ 68 Å in the [110] direction of the cubic box and twice as far in tetragonal box before they hit the boundary.

After initial equilibration at temperatures 1–50 K, an excitation of one atom (or more atoms) of the sample was performed by abruptly changing its (their) velocity (velocities). The case of initial excitation in the close-packed [110] direction was investigated most extensively. The time evolution of the kinetic energy and its equilibration process was studied for the shells containing all atoms of a perfect matrix that fall in the range $(n-1)R_{\mathrm{e}} < r < nR_{\mathrm{e}}$ For example, the first three shells consist of 12, 42 and 122 atoms, respectively. These shells

contain larger numbers of atoms than those of the crystallographic shells used in [4] whereby the strong fluctuations of thermodynamic quantities are widely suppressed.

The results of the 3D-MD calculations have been compared with approximate solutions of one-dimensional analytical models. It has been shown earlier that some aspects of heat transfer due to local excitation can be described quite well by a sequence of separate collisions along one-dimensional chains [4]. The approximate solution for a 1D chain of identical atoms interacting via a potential of the Born–Mayer type

$$V = A\ \exp(-x/a) \tag{1}$$

was given by Leibfried *et al* [37] in a model describing the energy redistribution in crystals after neutron scattering.

The transfer of spike energy into the crystalline environment can be derived from the relations describing the displacement of the nth atom

$$x_0(t) = v_0 t/2 - a \ln \frac{\cosh \zeta_1}{\cosh \zeta_0} \tag{2}$$

$$x_n(t) = v_0 t_1/2 + n\, R_e - a\ \ln \frac{\cosh \zeta_{n+1}}{\cosh \zeta_n} \tag{3}$$

$$\zeta_0 = \frac{v_0 t_1}{2a} \qquad \zeta_n = \frac{v_0}{2a}(t - n t_1) \tag{4}$$

$$t_1 = \frac{2a}{v_0} \ln \left[\sqrt{E_0/2A \exp(-R_e/a)} + \sqrt{E_0/2A \exp(-R_e/a) - 1}\ \right] \tag{5}$$

where $E_0 = m v_0^2/2$ is the impact energy of the atom (spike energy), and t_1 is the time between subsequent collisions. The solution represents a compressed longitudinal wave travelling along the 1D chain and, as was shown earlier [4, 27], properly describes atomic trajectories, pulse energy propagation as well as the Hugoniot plot, the latter relating 'pulse shock wave' and impact-atom velocities in the crystal [4].

3. Nature of ballistic heat current in dielectric crystals

The pulse shock waves transport the major part of the initial impact energy from the position of the energy spike into the bulk with supersonic velocity [4]. This ballistic energy transfer exceeds by far the normal heat conductivity in dielectric crystals [27].

As already mentioned above, the Leibfried 1D model properly describes kinetic energy transfer by shock pulses, but ignores the small dissipation caused by the interaction between the colliding atom and its neighbours. The transferred shock-pulse energy is thus constant and given by

$$E_{\max} = m v_0^2 \tanh^2(v_0 t_1/4a).$$

The small energy mismatch in the first collision

$$\Delta E = E_0 - E_{\max} = \sqrt{8 A E_0 \exp(-R_e/a)} \tag{6}$$

is due to the transfer of kinetic to potential energy of the shock (compression) wave.

The constant energy of the propagating pulse as well as the form of (3) point to the soliton character of the shock pulse. By replacing

$$\frac{v_0 t_1}{2a} \leftrightarrow \kappa \quad \text{and} \quad \frac{v_0}{2a} \leftrightarrow \beta \tag{7}$$

equation (3) takes the functional form of the well known 'Toda kink soliton' [26]

$$x_n(t) = a \ln \frac{\cosh \xi_{n-1}}{\cosh \xi_n} + \text{constant} \qquad \xi_n = (\kappa n + \beta t). \tag{8}$$

The solitary waves carry the energy

$$E_{\mathrm{T}} = a_{\mathrm{T}}/b_{\mathrm{T}}\,[\sinh(2\kappa) - 2\kappa] \tag{9}$$

where a_{T} and b_{T} are the parameters of the Toda lattice

$$V_{\mathrm{T}}(x) = a_{\mathrm{T}}/b_{\mathrm{T}} \exp(-b_{\mathrm{T}}\, x) + a_{\mathrm{T}}\, x.$$

As b_{T} is a dimensionless parameter, the lattice spacing is the unit length in the standard Toda soliton description. In order to enable comparison, the Leibfried and Toda lattice-potentials were fitted to each other by using the parametrization

$$A_{\mathrm{T}} = a_{\mathrm{T}}/b_{\mathrm{T}} = A \exp(-R_{\mathrm{e}}/a) \qquad b_{\mathrm{T}} = R_{\mathrm{e}}/a. \tag{10}$$

It can be easily shown that the soliton energy (9) is smaller than the Leibfried soliton energy E_0

$$E_{\mathrm{T}} < E_0 - A_{\mathrm{T}} \ln \frac{2E_0}{A_{\mathrm{T}}}$$

if the replacement (7) is used.

Leibfried and Toda 1D solitons carrying the same amount of energy, say $E_0 = 2$ eV, show slightly different behaviour; see figure 1. A Toda parameter $\tilde{\kappa}$ is calculated from (9) with $E_{\mathrm{T}} = E_0$ and used to evaluate the second parameter $\tilde{\beta} = \sqrt{a_{\mathrm{T}} b_{\mathrm{T}}/m}\ \sinh\tilde{\kappa}$ needed to determine the Toda soliton displacements (8). The main difference between the two kinds of kink soliton under discussion is given by $\Delta y = v_0 t_1$, the shift of the initial and final atomic displacements. This is shown in figure 1(a), where the atomic displacements of the Toda-kink solitons (broken lines) coincide with the Leibfried kinks (open points and solid line) shifted downwards by Δy (full points). The shift results from the difference in the initial conditions for both solitons. The Toda chain is compressed during the entire process of soliton propagation and the total displacement is equal to $y_{-\infty} - y_{\infty} = 2\tilde{\kappa}/b$ for the whole (infinite) lattice. The Leibfried chain is not compressed and the total displacement is zero. A local displacement (and local compression in the forward direction) is produced by the initial kinetic excitation of the central atom. Therefore, the initial position of the nth atom is given by $x_n(t_0) = nR_{\mathrm{e}}$ in the Leibfried case and by $x_n(t_0) = nR_{\mathrm{e}} - 2\tilde{\kappa}/b$ in the Toda case. On the other hand, atoms will finally relax to their equilibrium position $x_n(t_{\mathrm{f}} > nt_1) = nR_{\mathrm{e}}$ in the Toda lattice, but are shifted by $v_0 t_1 \approx 2\tilde{\kappa}/b$ to a new 'equilibrium position' in the Leibfried lattice, the latter resulting from the lack of an attractive part in the Leibfried potential.

The two solitons differ at times longer than $t > 7t_1$ (see figure 1), because in the considered case of equal excitation energies, $E_{\mathrm{T}} = E_0$, relation (7) is only approximately valid. The parameter $\tilde{\kappa}$ of the Toda soliton may be estimated from (9)

$$\tilde{\kappa} \simeq \ln\sqrt{2E_0/A_{\mathrm{T}}} \tag{11}$$

if $E_0/A_{\mathrm{T}} \gg 1$, i.e. $\sinh(2\tilde{\kappa}) \gg 2\tilde{\kappa}$. For a shock pulse of energy $E_0 = 2$ eV in Ar we have $E_0/A_{\mathrm{T}} \sim 150 \gg 1$. Under this condition, equation (5) can be simplified to

$$t_1 = 2a/v_0 \ln\left(\sqrt{E_0/2A_{\mathrm{T}}} + \sqrt{(E_0/2A_{\mathrm{T}}) - 1}\right) \simeq \frac{a}{v_0} \ln(2E_0/A_{\mathrm{T}}). \tag{12}$$

Together with the approximation (11) we arrive at

$$t_1 \simeq 2a\tilde{\kappa}/v_0. \tag{13}$$

This approximate relation for Toda and Leibfried solitons holds very well for a soliton-like shock pulse propagating through the Ar matrix with energies $E_0 > 0.5$ eV; see figure 1(b).

The velocity of the Toda soliton is given by the relation

$$c_{\mathrm{T}} = \tilde{\beta}/\tilde{\kappa} \tag{14}$$

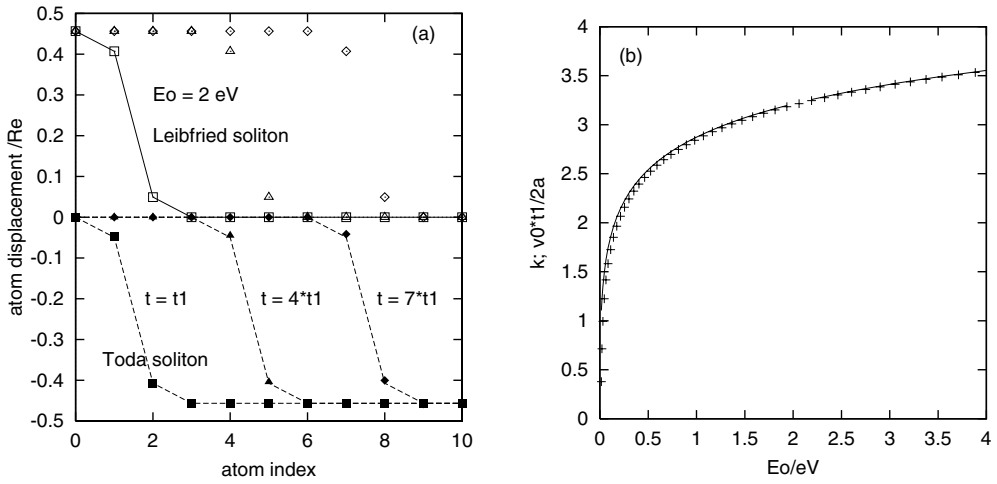

Figure 1. (a) Atom displacements for a soliton energy $E_0 = 2$ eV at times t_1, $4t_1$ and $7t_1$; Leibfried (open points and solid line) and Toda solitons (broken lines); the full points relate to the shifted Leibfried soliton. (b) The parameters $\tilde{\kappa}$ calculated from (9) (solid line) and $\kappa = v_0 t_1/2a$ (+), respectively; Leibfried and Toda lattice-potentials were fitted to the Ar potential given by Aziz *et al* [36], so $A = 8144.8$ eV and $a = 0.2679$ Å.

with

$$\tilde{\beta} = \sqrt{A_T b_T^2/m}\ \sinh\tilde{\kappa} \simeq b_T v_0/2.$$

By using (13) and (12) both c_T and the velocity of Leibfried solitons

$$c_L = R_e/t_1$$

obey the same relation

$$c_{T,L} \simeq \frac{v_0}{a/R_e \ln(2E_0/A_T)}.$$

Figure 2 presents the dependence of the compressed (shock) wave velocities versus the square root of its energy in the three cases under consideration. The exact relation (14) was used in the case of Toda soliton velocity (solid line). The agreement with velocity of Leibfried solitons (dotted line) is remarkable and confirms the above approximation. The marked points (Ar matrix) were obtained as averages over 30 different MD trajectories calculated for collision sequences initiated by impact energies of 2, 3.5 and 5 eV, respectively. As time evolves the energy decreases resulting in a series of points each related to the subsequent collision in the sequence. They all fall on a curve parallel to those found for the Leibfried and Toda lattices.

The observed shift is due to the fact that for the Ar lattice the shock velocity is plotted against the instantaneous kinetic energy, because in this case the potential energy of the compressed wave cannot easily be determined. However, if we consider the first collisions in each sequence, a plot versus the initial energy E_0 can be used resulting in a very good agreement between the 3D-Ar data and those of the 1D lattices. This is illustrated by the three marked points on the curves related to the Leibfried and Toda solitons. This correspondence together with the almost linear dependence $V_{sh} = V_{sh}(\sqrt{E})$ elucidates the solitary-wave character of the shock-wave pulse in the 3D-Ar crystal. Moreover, we have shown in [5] that colliding picosecond-shock waves in Ar crystals are stable objects.

The striking similarities of the energy transfer behaviour of the shock waves observed in the real 3D system and in the two 1D models originate from the 'focusing effect' [33]

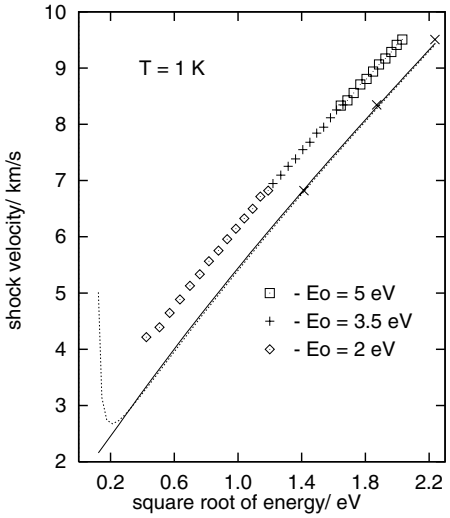

Figure 2. Compressed wave velocities in 3D-Ar (◇ and +) and for the 1D lattices according to Toda (solid line) and Leibfried (dotted line).

referred to in the introduction. The latter results in a selective choice of the [110] direction (the one with the closest interparticle distance in fcc crystals), along which the propagation of the 'solitary shock waves' is most effective. Moreover, we note that the profile as well as the velocity of the soliton-like pulses are mainly determined by the repulsive part of the potential (the only interaction in the Leibfried model). It was left unchanged in all models discussed in the present paper. The coupling of propagating soliton-like pulses with the surrounding [110] chains (in 3D) is weak. Considering these stochastically varying interactions as 'external' the situation resembles that discussed by Hu *et al* [16, 19] in their study of heat conduction in 1D chains with an external on-site potential. The weak coupling to the surroundings is the source of soliton-energy dissipation (see section 4), which may even be suppressed by a proper choice of excitation conditions as discussed in section 5.

4. Ballistic heat (energy) transfer in dissipative media

Dissipation causes a decrease of the soliton energy and diminishes the ballistic contribution to the heat current [3]. On the other hand, the ballistic contribution increases by enlarging the temperature gradient [3]. The monatomic lattice with one or (two) initially excited atom(s) is a special case where the requirements for significant ballistic contribution are well fulfilled. As examples we refer to photodissociation of matrix-isolated molecules or nonradiative exciton quenching in rare-gas solids. In both cases the kinetic energies set free by initial excitation can be fairly high (up to 5 eV) and the 'thermal' (kinetic energy) gradients may exceed 10^4 K Å^{-1} or 10^{14} K m^{-1} in solid Ar.

Firstly, we will study the ballistic heat transport and its time evolution under the favourable conditions in a pure Ar matrix. The less favourable case, energy transfer initiated by a light defect atom will be discussed below in section 4.2.

4.1. Energy transfer in monoatomic crystals [4, 38]

It was shown in [4] that very fast energy transfer takes place in a monatomic lattice after local excitation of an atom (few atoms) in the matrix. The heat (energy) current emanates from the excitation centre by means of one or more supersonic, solitary pulses along the various [110]

directions. The number of pulses depends on the initial direction and e.g. equals 1 for initial excitation in the [110] direction or 4 for excitation close to the [100] direction.

The initial energy (heat) current

$$J = (E_0/V_u)V_{sh} \tag{15}$$

($V_u = 37.4$ Å^3 is the volume of the unit cell) then reaches values $J = 12.7$ eV Å^{-2} ps^{-1} $\sim 2 \times 10^{11}$ kJ m^{-2} s^{-1} for $E_0 = 5$ eV, $V_{sh} \sim 95.1$ Å ps^{-1}. As the pulses move, their energies gradually dissipate due to interaction with the environment [38].

Figure 3 presents the pulse-energy dissipation for initial excitation in the [110] direction at energies $E_0 = 1, 2, 3.5$ and 5 eV, respectively. The evolution of the pulse energies for 30 different MD trajectories are marked by different symbols. The solid line connects energy values averaged over these trajectories; the dashed–dotted curve corresponds to values obtained from the modified 1D Leibfried model (1D-mLM) presented in [38].

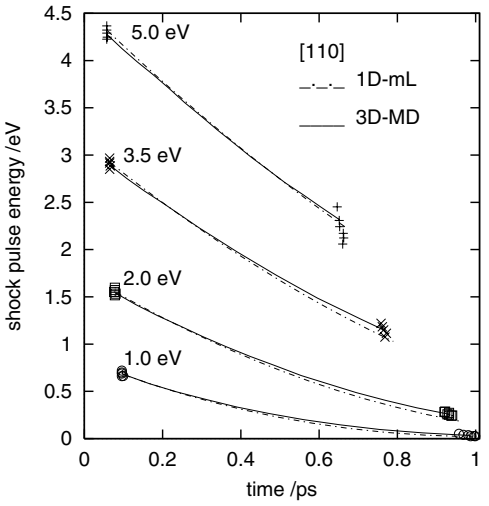

Figure 3. Pulse energy versus time; excitation along the [110] direction.

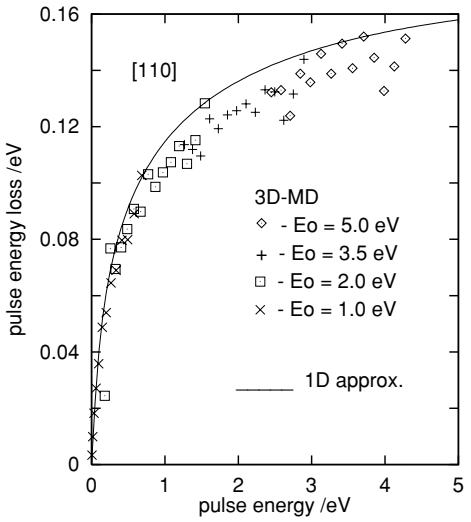

Figure 4. Energy loss per collision for different excitation energies; sequence of 14 collisions.

The amount of energy transferred to the atoms located next to the propagation path in each step of the collisional sequence is shown in figure 4. Each point represents an average over 3D-MD trajectories for each of the 14 collisions in every sequence and for several excitation energies. The amount of pulse energy dissipated in each collision increases with its energy in an almost monotonic manner and slowly saturates at 0.14 eV for $E_0 > 4$ eV, which agrees well with $\Delta E_d \sim 0.12$ eV, a value estimated by Cui *et al* [31]. The dependence discussed above also matches with the results of the 1D model [38] shown as a solid line in figure 4. We thus conclude that compressed waves in the 3D-Ar crystal dissipate energy mainly due to interactions with the four atoms located next to the propagation path (the closest neighbours of the [110]-chain atoms). In the 2D model there are only two such atoms and there are none in 1D lattices. Therefore we conclude that a decrease of the lattice dimension diminishes dissipation and results in a increase of the ballistic contribution to the heat current.

This can be related to the FPU-chain results of Hu *et al* [19] according to which the energy transport mechanism changes from transfer assisted by solitary waves to a diffusive process

by increasing the on-site potential. This corresponds to the increased number of interacting neighbouring atoms in the case studied.

Since the modified Leibfried model [37] describes pulse propagation properly, we suggest a quantitative description of the heat transport by incorporating into the sequence of independent binary collisions the stepwise dissipation of soliton-like pulses. In the case where the initial impact is in the [110] direction, the instantaneous ballistic current is given by

$$J = E_n / V_u V_{sh}(E_n) \tag{16}$$

where E_n, the instantaneous kinetic energy at the nth collision, is calculated by subtracting from E_{n-1} interactions with lateral atoms as discussed above and displayed in figure 3.

We have shown that the dissipation increases (the ballistic heat current decreases), when the direction of the initial impact deviates from the [110] direction. The effect is most pronounced for the first two collisions in the sequence. Later, after a few collisions, the well known 'focusing effect' [33, 37] imposes alignment of the pulse propagation along the [110] direction (close-packed in fcc crystals).

Raising the matrix temperature disturbs the alignment of collision processes and the directed transfer of collision energy, thus enhancing the lateral energy dissipation. Therefore the pulse energy decreases more rapidly at higher temperatures (see figure 5).

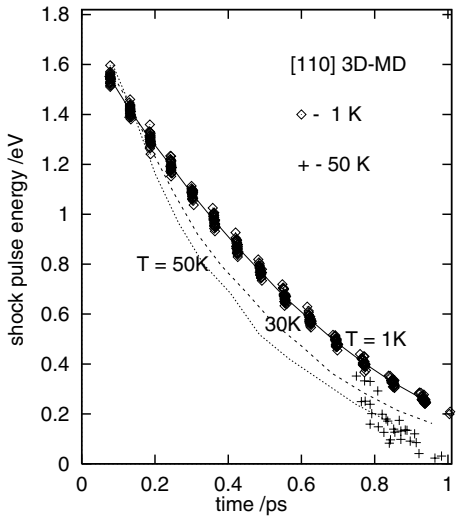

Figure 5. Temperature dependence of pulse-energy dissipation; solid and broken curves connect averaged energy maxima for a crystal at chosen temperatures.

As illustrated by a selected set of points representing 30 different MD trajectories at 1, 30 and 50 K, we also learn that the dispersion of pulse energies increases at higher temperatures.

Thus, the ballistic contribution to the heat transfer decreases on raising the matrix temperature, in contrast to the diffusive part. There is a similar temperature dependence of the thermal conductivity in figure 4 of [19] for the energy transport assisted by the solitary waves. At low temperature the heat conductivity of dielectric materials usually grows with an increase of T; see [28].

4.2. Energy transfer initiated by a light defect atom

It was argued in [30] that—in the case of energy transfer initiated by a light defect atom—the ballistic contribution will be suppressed as a result of many chaotic collisions as well as a reduced energy transfer per collision; both effects enhance the diffusive part of heat transfer. To clarify whether these assumptions hold true, we studied [27] the energy transfer emerging from excitation of a light impact atom ($m_0/M_{\mathrm{Ar}} = 1/40$) in an Ar lattice. We have focused attention on energy transfer between the impact atom and the host atoms of the first shell, since beyond this region pulse propagation will proceed according to the picture just given. The relation between the resulting energy transfer and the normal (Fourier) conductivity law will now be discussed.

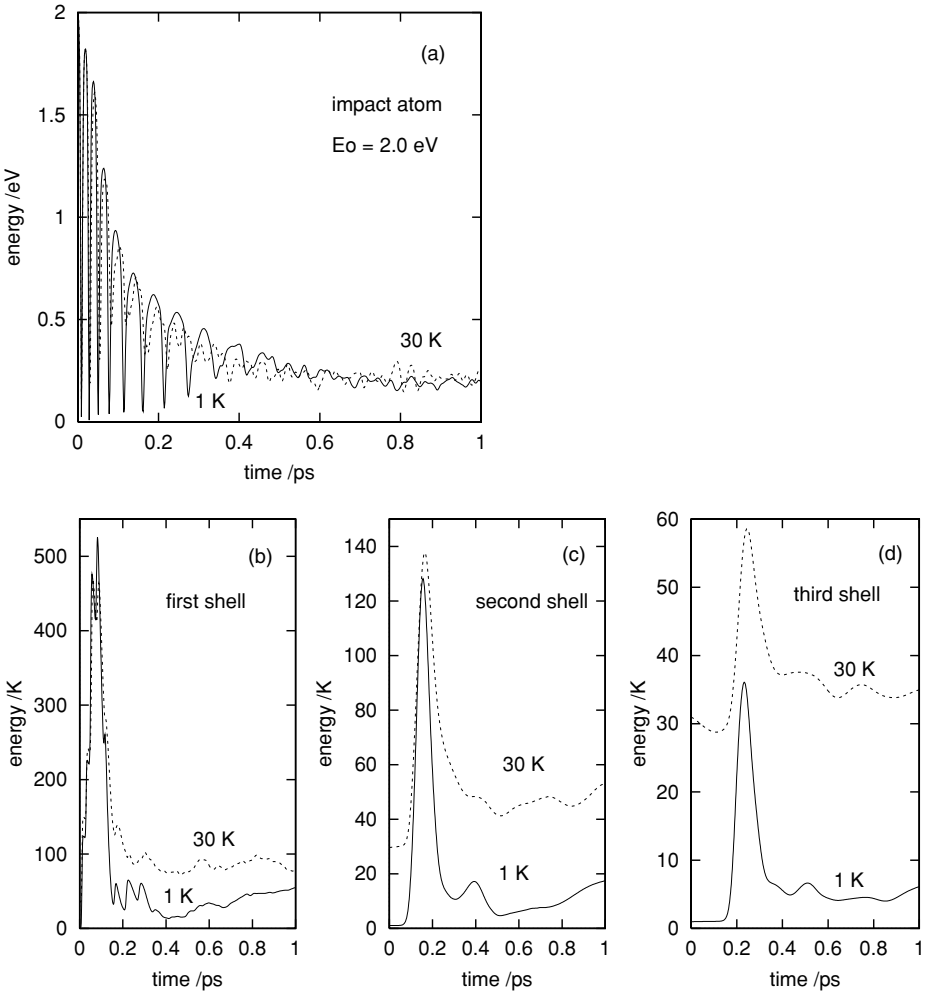

Figure 6. (a) Time evolution of the light impact-atom energy; (b)–(d) mean kinetic energy of the atoms in shells $n = 1, 2$ and 3, respectively; Ar-matrix temperature 1 K (full line) and 30 K (dashed line).

Figure 6 displays the evolution of kinetic energy (and its mean shell values) for the light impact atom and the atoms comprised in the first three shells at lattice temperatures 1 and

30 K and $E_0 = 2$ eV. The collision sequence proceeds along the [110] and [$\bar{1}\bar{1}$0] directions. Initially, the excitation energy relaxes slightly faster at temperature $T = 30$ than at 1 K. At times $t > 0.6$ ps, the kinetic energy curves for both temperatures merge at a level of 10% of E_0 (0.2 eV), an energy well above the thermal energy of the crystal; figure 6(a). Figure 6(a) also shows that the energy transferred in the first two collisions is approximately equal to 0.18 eV, which fits well with the value of 0.19 eV calculated from

$$\Delta E_0 = 4E_0\, m_0 M_{\mathrm{Ar}}/(m_0 + M_{\mathrm{Ar}})^2. \tag{17}$$

Equation (17) results from the solution of the modified 1D-Leibfried model (allowing for different masses of the collision partners):

$$x_n(t) = \frac{m_0}{m_0 + M_{\mathrm{Ar}}}\, v_0 t_1 + n\, R_{\mathrm{e}} - 2\, a \frac{M_{\mathrm{Ar}}}{m_0 + M_{\mathrm{Ar}}}\, \ln \frac{\cosh \zeta_{n+1}}{\cosh \zeta_n}. \tag{18}$$

The increase of the energy transfer rate in the third collision ($39 < t < 65$ fs); see figure 6(a), is remarkable, especially in comparison to the significant decrease of the impact-atom energy caused by the previous interactions. This increase of transfer rate is presented in figure 6(b) as a third shoulder on the kinetic energy pulse of the first-shell atoms. Two smaller shoulders of an otherwise smooth curve are followed by a significantly larger change of the first-shell energy, although energy transfer to the second shell has already started (figure 6(c)). This results from the coherent motion of several [110]-chain atoms as was explained in [27].

We have also studied in which manner the ballistic energy transfer caused by light-atom excitation is affected by varying the direction of the excitation. We have chosen the three high-symmetry directions ([110], [111] and [100]) where two, six and eight almost equi-energetical solitary pulses travelling along equivalent closest-neighbour directions are excited. In a previous paper [4] we have shown that atoms residing in equilibrium sites at distances nR_{e} from the excitation centre are more strongly excited than the others. This finding was independent of the excitation direction, which led us to the conclusion that the solitary pulses predominantly propagate along the crystallographically equivalent [110] directions. The symmetry of the system allows us further to state that, e.g. in the case of [100] excitation four pulses will propagate in the forward and four in the backward longitudinal direction. By initially exciting along a low-symmetry direction (here [631]) we give preference to one of those solitary pulses lying closest to the excitation direction by transferring more energy to it. This widens the spread of generated pulse energies.

Figure 7 shows the energy pulse consisting of many of these solitary pulses propagating through the first three shells. Ballistic transfer is still present even in the low-symmetry case. Broadening of the pulse widths together with a slowing down of the pulse velocities indicate that a growing number of solitons with different velocities is propagated through the crystal. This is shown in figure 7 for excitation in the [110], [111], [100] and [631] direction, respectively. The widths of the energy pulses transmitted through the second shell (figure 7(b)) are 0.093 ps (determined at 86.6 K), 0.127 ps (at 81.2 K), 0.156 ps (at 77.5 K) and 0.157 ps (at 73.0 K) for these four directions, respectively. The pulse widths broaden on proceeding from shell to shell, e.g. for [631] we have 0.117, 0.157 and 0.23 ps for the first, second and third shell, respectively. The velocity changes are due to dissipation. The pulse velocities in the third shell are 45.6, 28.8, 26.7 and 24 Å ps^{-1} (all $\pm 10\%$) for the excitation directions mentioned above. We thus conclude that by increasing the number of propagated solitary pulses the ballistically transferred amount of energy and the transfer velocity is reduced, whereas energy pulse dispersion gets larger. Moreover, our results show that, in the range where ballistic energy transfer is significant, the applicability of spherically symmetrical models based only on diffusive type transport [30] is hardly justified. Since the major part of energy is carried by

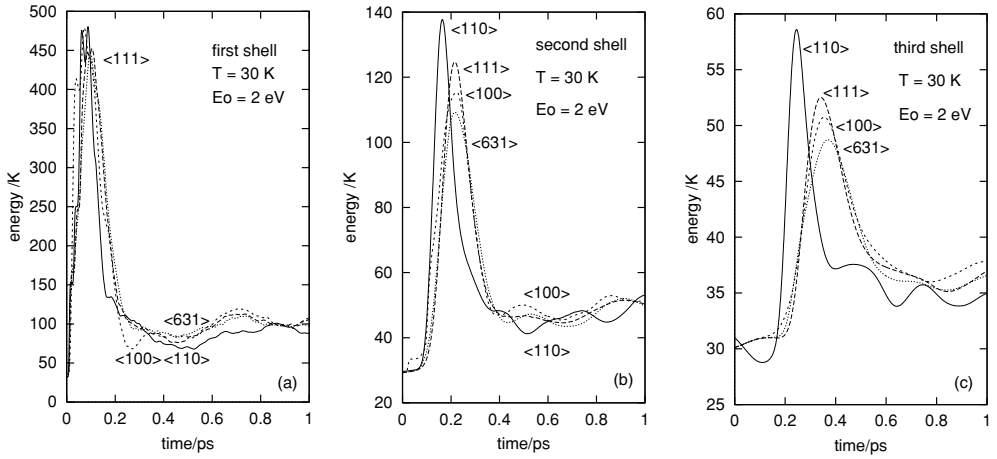

Figure 7. Time evolution of the mean kinetic energy of the first three-shell atoms for various excitation directions [111], [110], [100] and [631].

one pulse or a few high-energy solitary pulses propagating along the equivalent [110] crystal directions, the short-time energy propagation reveals a large spatial anisotropy.

5. Means to suppress the ballistic current dissipation

The suppression of soliton energy dissipation is of great theoretical and technical importance. It was mentioned in section 4.1 that dissipation is caused by the interaction of the colliding atom with the atoms lying close to the propagation path. This led us to investigate means of dissipation suppression by introducing modified guest–host interactions and different excitation conditions. In this context, we first studied solitary pulse propagation along a close-packed [110] chain of guest atoms of masses $M = 131$ (Xe) and $M = 4$ (He) embedded in an Ar host lattice and found that the energy loss does not depend on the masses of the impurities significantly.

5.1. Coherent excitation of an atomic complex

In order to study the impact of an extended atomic complex, we have excited coherently the centre atom $A_1(0, 0, 0)$ and its four neighbour atoms $B_{1i}(1/2\ a_{Ar}, 0, \pm 1/2\ a_{Ar})$ and $(0, 1/2\ a_{Ar}, \pm 1/2\ a_{Ar})$, $i = 1, \ldots, 4$, which lie ahead of A_1 as it moves in the [110] direction of an Ar (fcc) crystal. Figure 8(a) displays the evolution of the kinetic energy of the centre atom caused by exciting the five-atom complex at energies of 5×1.0 and 5×3.5 eV. During the first collision the central chain loses part of its kinetic energy while the potential energy is enhanced (local compression of the chain). Later, the central chain remarkably regains almost all of its initial kinetic energy. What is the mechanism underlying the internal energy exchange between the parallel A_n and B_{ni} chains?

When the B_{1i} atoms move forward they interact with the atoms of the parallel chains including the atom $A_2(1/2\ a, 1/2\ a, 0)$ of the central [110] chain. Thus, the coherent motion of B_i neighbours favours the propagation of energy along the A_n chain in a twofold way:

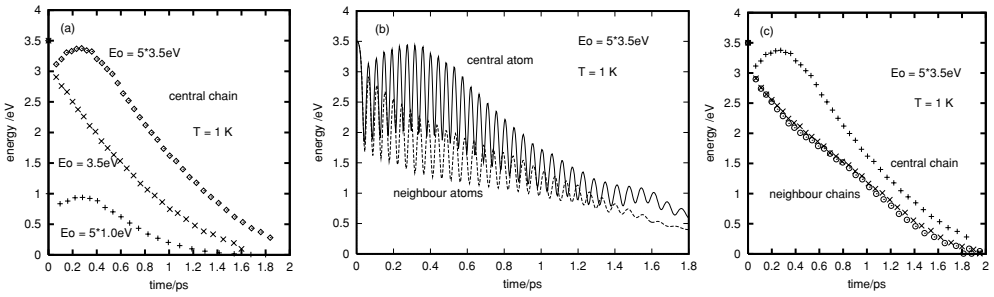

Figure 8. Kinetic energy of central A_n chain and neighbouring chain atoms B_{ni}; (a) energy maxima of the central chain atoms versus time. Complex excitation energies $E_0 = 5 \times 1.0$ (+) and 5×3.5 eV ($\diamond$); marks ($\times$) represent the energy maxima for the one-atom excitation at $E_0 = 3.5$ eV; (b) energy exchange between central chain (solid line) and neighbouring chains (broken line), (c) energy maxima of A_n chain (+) and of two selected B_{ni} ($\times$, $\odot$) chains versus time.

(i) the A_1 atom loses less energy because the closest B_i neighbours move in phase;
(ii) the adjacent A_2 with which the A_1 atom collides has already gained initial kinetic energy by interacting with the four B_{1i} neighbours.

The kinetic energy of atom A_3 is thus enhanced to a value higher than that of A_2; see figure 8(a), an effect which continues to occur in the next few collisions. However, since the A_n chain atoms gradually gain energy, the respective pulse propagation velocities increase (they are proportional to the square root of the soliton energy). Finally, the pulse travelling along the A_n chain overtakes the pulses propagating along the B_{ni} chains. Note that the B_{ni}-chain pulses have already slowed down due to interaction with their closest neighbours. At this stage the energy dissipation of the A_n atoms is similar to the case of one-chain excitation (see curve '$\times$' in figure 8), as the interacting neighbours are now at rest.

The quite rapid energy drop of the central chain atoms results from increased energy losses to the neighbouring atoms. In the region where 12th to 20th collisions took place, the slightly smaller energy loss of the B_{ni} atoms is related to the motion of the A_n atoms now moving ahead of the B_{ni} atoms. One can expect that the effect will be stronger if other parallel A_{ni} chains are excited as well. As a result a continuous energy exchange between the A_{ni} and B_{ni} chains will occur as discussed in section 5.2. In the present case, the exchange is generally restricted to the initial enhancement of the pulse carried by the A_n chain. This is merely due to the fact that the B_{ni} pulses will never again overtake the A_n pulse. Although the central chain pulse will slow down as well, the time delay between the pulses carried by the A_n and B_{ni} chains increases. This can be seen from figure 8(c), taking into account the time difference between the points representing energy maximum at the last considered atoms ($n = 36$th) in the chains: for central (+) and neighbour chains ($\times$ and $\odot$). The A_{36} atom reaches its energy maximum about 200 fs before $B_{i,36}$. This is equivalent to two collision times in the given energy region. Therefore central pulse enhancement will not appear again. The energy remaining in the chains (see figure 8(b)), is still confined in chains and far from the thermal equilibrium value. Notice, moreover, that the coherence of the motion of the atoms in neighbouring chains is completely destroyed after 1 ps. Similar results were found, if the atoms of the primary complex are initially excited at different energies.

We finally conclude that pulse propagation enhancement (dissipation suppression) is supported in a system where the A_{ni} and B_{ni} chains exchange energy continuously and similarly to the initial-stage process just described above. Since the border atoms of the excited complex suffer the largest energy loss, we can expect energy exchange between the chains to

increase and dissipation to decrease, if the excitation volume is extended. The extreme case is the excitation of an infinite complex i.e. two planes carrying A_{1i} and B_{1i} atoms.

5.2. Planar excitations

Figure 9 presents the time dependence of the average kinetic energy emerging from [110]-directed excitation of two adjacent planes of A_{1i} and B_{1i} atoms, respectively. The continuous energy exchange between 'solitary plane excitations' can be observed with dissipation strongly suppressed. This results from the fact that the dominant dissipation source, namely interaction with surrounding atoms (interaction with a bath for a solitary pulse) leads now to energy exchange between the planar excitations. The mechanism was discussed above in section 5.1 with the exception that the energy transfer between planes proceeds in cycles with a period of about 0.6 ps as shown in figure 9.

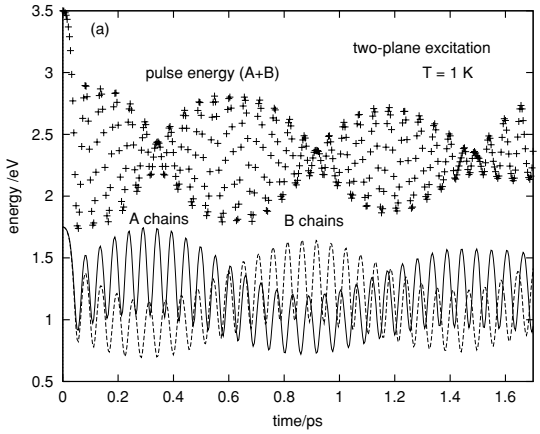

Figure 9. Time evolution of the average kinetic energy per atom; excitation of A (solid curve) and B (broken curve) planes in [110] direction; the marks + show the evolution of the pulse energy in (A + B) chains; excitation energy per atom 1.75 eV.

The only contribution to pulse energy loss is the interaction with the chain atoms left behind the propagating front. Taking into account that during 35 collisions the chain atoms have dissipated roughly 0.16 eV we have an average loss per collision of 4.6 meV which is much smaller than for one-atom excitation ($\sim$ 140 meV). Again, the initial drop in kinetic energy ($\sim$ 0.3 eV per atom) results from kinetic to potential energy transformation.

The importance of energy exchange between the two planes is also made evident in figure 10, where the kinetic energy evolution produced by one- and two-adjacent plane excitation with the same total energy is shown. Obviously, the energy dissipation is not greatly influenced by increasing the number of excited chains (according to figure 10 one-atom excitation may be even advantageous). However, excitation of the two adjacent planes suppresses dissipation very effectively.

We conclude that the two-plane excitation allows one to drastically reduce (or even eliminate) dissipation to the closest-neighbour chains parallel to the [110] directions, whereas energy loss due to interaction with the atoms left behind the excitation front (usually a less effective dissipation channel) is not significantly affected. The latter amounts to roughly 10 meV, when the first atom is excited with an energy of 2 eV. It seems that one possible way to diminish this dissipation channel is to initiate excitation by local compression as in the Toda

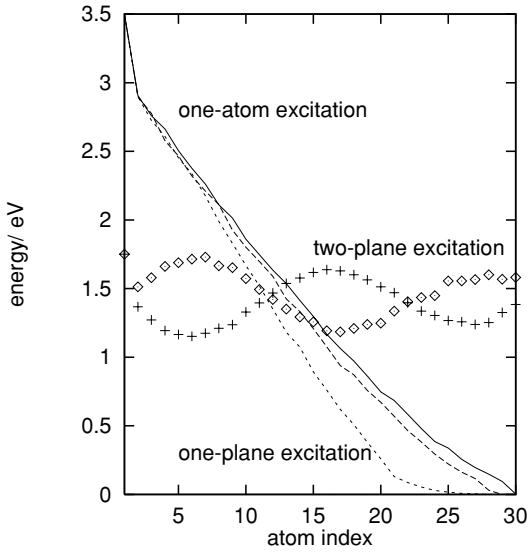

Figure 10. Comparison of one- and two-plane as well as one-atom excitations; the dashed–dotted lines present kinetic energy drop in various chains after one-plane excitations and the solid line connects the kinetic energy maxima after one-atom excitation, both with energy 3.5 eV per chain; energy evolution after two-plane excitation (1.75 eV per chain) is marked by ◇ and +.

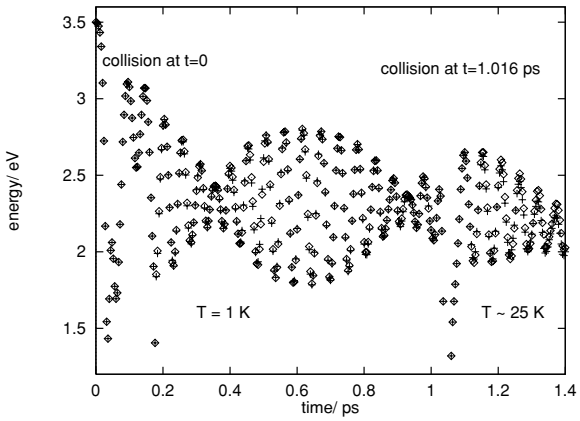

Figure 11. Collisional stability of two colliding energy pulses each created by two-plane excitation; pulse energies per A_{ni} chain are marked by + and ◇ for the two colliding pulses.

lattice. The post-collision position of the atom is then its lattice equilibrium position without any vibration, as in our case.

The redistribution of excitation energy between the A_i and B_i chains or coherent excitation of more than two planes contributes to dissipation suppression less well.

The energy pulses created by two-plane excitation preserve the solitonic character of the single-atom shock wave, e.g. it is robust against the collision. Figure 11 presents the pulse energy per chain of two pulses propagating in opposite [110] directions and being started at adjacent atoms. After collision at time $t = 0$ the pulses propagate coherently further. Due to the periodic boundary conditions applied in our MD calculations, they collide (after 1 ps) and recover again. However, since they propagate through a crystal of higher temperature

($T \sim 25$ K), they lose their perfect coherence. Dissipation increases significantly in relation to the time before the second collision.

6. Conclusions

We have shown that the ballistic heat (energy) transfer in solid Ar significantly contributes to the heat flux emanating from an energy spike generated e.g. by the dissociation of a guest molecule or by exciton quenching. The ratio of ballistic to diffusive current in the energy stream decreases along the propagation path and vanishes at distances of the order of 100 R_e. The ballistic heat current is equivalent to a propagating series of femtosecond pulses (pulsed shock waves) and may be considered as a sequence of Leibfried–Toda (LT) solitons travelling through the dissipative medium. These shock pulses display all important characteristics of solitons, i.e. they are collisionally stable and their velocities are proportional to the square root of the transferred energy (in contrast to phonons).

The ballistic contribution to the heat current decreases with the distance from the excitation centre because of energy dissipation of the soliton-like pulses. These energy losses increase with the number of neighbouring atoms met along the propagation path, the latter depending on the impact direction and system dimension. The energy loss reaches a minimum for 1D systems as surmised to be the case in [24]. Energy transport along the [110] direction in the fcc crystal may be treated as 1D energy transfer with an on-site potential created by the interactions with atoms lying in neighbouring chains. It was shown by Hu *et al* [16, 19] that such interactions not only decrease the ballistic contribution but also induce normal heat conduction in 1D lattices.

The ballistic, soliton-like propagation along close-packed directions of the crystal is highly directional and hardly compatible with the symmetrical heat transfer emanating from a point heat source. Energy (heat) propagation lateral to the direction of excitation is much smaller than that in the radial direction, at least in the ballistic propagation range. The situation is slightly improved for higher lattice temperatures and for excitations caused by small impact atoms.

The same features of energy transfer can be expected for all noble gases and other regular crystals with significantly stronger interactions in the preferred directions. The ballistic contribution to the heat transfer decreases, however, with the crystal temperature increase (worse atom alignment along the chosen direction) similarly to the heat conductivity in [19]. In contrast to the diffusive part, the ballistic contribution to heat transfer decreases by increasing the temperature.

Furthermore, we have proven that coherent many-atom excitation may, if properly devised contribute to the lifetime increase of the TL-solitons. Excitation of an atom together with its closest neighbours may increase the pulse propagation range. The method is, however, energetically inefficient. The situation is even worse in case of one-plane excitation. However, excitation of two neighbouring planes significantly increases the propagation range of the solitons. This results from the interaction of the planes and a dissipation decrease at the solitary wave boundaries. Excitation of three adjacent planes as well as mass-diversification of the propagating chains do not lead to further suppression of dissipation.

The two-plane excitation allows one to eliminate (or at least drastically reduce) dissipation to the neighbouring chains in [110] directions. However, it leaves the energy loss which is due to interaction with the atoms left behind the excitation front unaffected. One possible way to decrease this dissipation channel is to start the excitation by local compression as in a Toda lattice.

Acknowledgments

This work was sponsored by Deutsche Forschungsgemeinschaft via Sfb 337. AC gratefully acknowledges the hospitality of the Physics Department of the FU Berlin.

References

[1] Jackson E A and Mastriotis A D 1989 *J. Phys.: Condens. Matter* **1** 1223
[2] Nishiguchi N, Kawada Y and Sakuma T 1992 *J. Phys.: Condens. Matter* **4** 10227
[3] Ohtsubo Y, Nishiguchi N and Sakuma T 1994 *J. Phys.: Condens. Matter* **6** 3013
Ohtsubo Y, Nishiguchi N and Sakuma T 1993 *Japan. J. Appl. Phys.* **32** 2256
[4] Cenian A, Hennig S and Gabriel H 1995 *J. Chem. Phys.* **102** 9276
[5] Cenian A, Gabriel H and Hennig S 1996 *J. Tech. Phys.* **37** 291
[6] Poetzsch R H H and Boettger H 1998 *J. Phys.: Condens. Matter* **10** 943
[7] Born M 1914 *Phys. Zeitschr.* **15** 191
[8] Debye P 1914 *Vorträge über die kinetische Theorie* (Leipzig: Teubner)
[9] Peierls R 1929 *Ann. Phys.* **3** 1055
[10] Fermi E, Pasta S and Ulam S 1955 *Los Alamos Scientific Laboratory Report* LA-1940
[11] MacDonald D M K 1958 *Proc. Int. Symp. on Transfer Processes in Statistical Mechanics, Brussels* ed I Prigogine (New York: Wiley)
[12] Casati G, Ford J, Vivaldi F and Visscher W M 1984 *Phys. Rev. Lett.* **52** 1861
[13] Lepri S, Livi R and Politi A 1998 *Europhys. Lett.* **43** 271
[14] Lippi A and Livi R 2000 *J. Stat. Phys.* **100** 1147
[15] Prosen T and Campbell D K 2000 *Phys. Rev. Lett.* **84** 2857
[16] Hu B, Li B and Zhao H 1998 *Phys. Rev.* E **57** 2992
[17] Hatano T 1999 *Phys. Rev.* E **59** R1
[18] Prosen T and Robnik M 1992 *J. Phys. A: Math. Gen.* **25** 3449
[19] Hu B, Li B and Zhao H 2000 *Phys. Rev.* E **61** 3828
[20] Tsironis G P, Bishop A R, Savin A V and Zolotaryuk A V 1999 *Phys. Rev.* E **60** 6610
[21] Gendelman O V and Savin A V 2000 *Phys. Rev. Lett.* **84** 2381
[22] Giardini C, Livi R, Politi A and Vassalli M 2000 *Phys. Rev. Lett* **84** 2144
[23] Li B, Zhao H and Hu B 2001 *Phys. Rev. Lett* **86** 63
[24] Lepri S, Livi R and Politi A 1997 *Phys. Rev. Lett.* **78** 1896
[25] Toda M 1979 *Phys. Scr.* **20** 424
[26] Toda M 1981 *Theory of Nonlinear Lattices* (Berlin: Springer)
[27] Cenian A and Gabriel H 1996 *Proc. III Int. Forum of Heat/Mass Transfer, Minsk* ed B A Kolovandin, V A Sosinivich, V A Tziganov, T V Sidorovich (Minsk: Heat and Mass Transfer Institute) part I, p 13
[28] Carruthers P 1961 *Rev. Mod. Phys.* **33** 92
[29] Wolfe J P 1980 *Phys. Today* **33** 44
Northrop G A and Wolfe J P 1979 *Phys. Rev. Lett.* **43** 1424
[30] Tarasova E I, Ratner A M, Stepanenko V M, Fugol I Ya, Chergui M, Schriever R and Schwentner N 1993 *J. Chem. Phys.* **98** 7786
[31] Cui S, Johnson R E and Cummings P 1988 *Surf. Sci.* **207** 186
[32] de Pujo P and Mestdagh J-M 1993 *Z. Phys.* D **25** 357
[33] Silsbee R H 1957 *J. Appl. Phys.* **28** 1246
[34] Borrmann A and Martens C C 1995 *J. Chem. Phys.* **102** 1905
[35] Kunttu H, Feld J, Alimi R, Becker A and Apkarian V A 1993 *J. Chem. Phys.* **98** 7786
[36] Aziz R A and Slaman M J 1986 *Mol. Phys.* **58** 679
[37] Leibfried G 1965 *Bestrahlungseffekte in Festkörpern* (Stuttgart: Teubner) p 219
[38] Cenian A, Hennig S and Gabriel H 1996 *Proc. Femtochemistry: The Lausanne Conference*, *1995* ed M Chergui (Singapore: World Scientific) p 623